Energy Reports 14 (2025) 1479–1490

Contents lists available at ScienceDirect

Energy Reports

journal homepage: www.elsevier.com/locate/egyr

Research paper

Experimental analysis of installing multirotor horizontal wind turbines in a ducted wind turbine: The influence of rotor diameter and rotation on power efficiency optimization

Javad Taghinezhad [a], Mehran Masdari [b,*], Mohammad Omidyeganeh [b]

[a] Faculty of Engineering & Technology, University of Tehran, Tehran, Iran
[b] School of Science & Technology, City St George's University of London, London, United Kingdom

ARTICLE INFO

Keywords:
Renewable energy
Ducted wind turbines
Experimental test
Multi-rotor turbine
3D surface analysis
Optimization

ABSTRACT

The current study focuses on applying duct and multi-rotor wind turbines to enhance the generating capacity of a wind system arrangement in response to the expanding enthusiasm for using renewable energy sources in the municipal area. The outcome of this research can be utilized to introduce optimal turbine arrangements for a range of wind speeds related to specific regions to optimize the amount of power that can be extracted. It can produce power on standalone or in collaboration with other systems, such as Airborne and Invelox configurations. A duct speeds up the wind flow through the turbine location, while additional turbines can capture the remaining energy in the turbine's wake. For this aim, the impact of various configurations of multi-rotor wind turbines mounted on a recently designed duct was explored, followed by an investigation into enhancing the total output power. The effect of rotating direction and rotor diameter has been examined by comparing multiple arrangements to achieve the most significant output power for wind speeds ranging from 4 to 16 m/s. The outcomes prove that in high-speed winds of 12 m/s or more, mounting one rotor with a smaller diameter in the middle of two larger ones within the duct while spinning in the counter-rotating situation enhances the power efficiency by up to 95 %. Moreover, in low-speed winds of 6 m/s or lower, the three rotors with the same diameters presented the highest output, almost 2.1 times compared to the single rotor mounted in the duct throat. Considering an appropriate arrangement for multirotor wind turbines regarding privileged wind speed in the region can significantly increase generated power.

1. Introduction

To reach sustainability and minimize the impacts of climate change, nations all over the world are taking steps to use renewable energy sources instead of conventional power generated from fossil fuels (Ouyang et al., 2024). Plenty of countries are implementing a framework for energy transition and minimizing emissions of pollutants (Shen et al., 2024). Wind energy, as a source of green energy, can adequately mitigate the utilization of carbon-based fuels and emissions of greenhouse gases, and it is recognized as an affordable source of clean energy (Amiri et al., 2024). Wind turbines are the primary tools used to capture wind energy. The energy generated by wind has not yet reached its maximum potential; however, traditional wind turbines have expanded steadily during the last twenty-year period. Large wind turbines with greater blades and more elevated towers were built; due to this development, the cost of manufacturing, maintenance, and repairs has risen. These wind turbines face the cost of transmitting electricity. Additionally, the upstream wind turbines' wake in large-scale power plants decreases the wind velocity. It creates a turbulent flow in their wake, (Akhtar et al., 2024; Kim et al., 2015) which can reduce output power (Dou et al., 2019).

The main focus of recent studies in the wind energy field is reducing the overall cost of generating electricity due to the fast growth of wind technology (Tao et al., 2024; Song et al., 2018a, 2018b). According to technical terms, the objective is attempting to capture the wind as well as possible (Cao et al., 2024). Various subjects are investigated and considered, such as optimizing wind turbine aerodynamics, (Tayebi and Torabi, 2024; Mangano, 2023) assessing power curves in several scenarios (Spiru and Simona, 2024; Yesilbudak and Ozcan, 2024; Qiao et al., 2024), improving blade shape, (Qian et al., 2024; Firoozi et al.,

* Corresponding author.
E-mail address: mehran.masdari@city.ac.uk (M. Masdari).

https://doi.org/10.1016/j.egyr.2025.07.029

Available online 29 July 2025

2024; Li et al., 2024) and boosting the wind farm's total output by relocating wind turbines (Gao et al., 2016; Hu et al., 2024; Tian et al., 2024). Additionally, they developed novel wind-capturing innovations, including Invelox, (Aravindhan et al., 2024; Heidari et al., 2024) Air-borns, (Schmidt et al., 2024; Bayati, 2024) and ducted wind turbines (Taghinezhad et al., 2024; Mozafari et al., 2024). This current study provides an in-depth assessment of multi-rotor ducted wind turbines to complete the previous research on ducted wind turbines (Taghinezhad et al., 2021a).

In the past few years, the development of duct-mounted turbines for low-functional wind technologies has been investigated as an affordable approach (Akhter et al., 2024). Many scientists have made an effort to enhance the operational efficiency of these sorts of wind turbines. Allaei (Allaei and Andreopoulos, 2013, 2014; Allaei, 2012) established the INVELOX, a type of ducted wind turbine that produced power using a throat shape similar to a venturi and an airflow-gathering section. Their study findings predominantly concentrated on the simulation and construction of flow ducts. Their last investigation evaluated the experimental effects of adding two or three propellers in the duct throat area (Allaei et al., 2015). Many researchers have worked on different parts of Invelox to expand its performance; for instance, (Ayaz et al., 2023) developed the structure of funnel and venturi parameters to improve the power generation capacity and reported that they improved it by 3.2 times compared to the original concept. Some others (Heidari et al., 2024; Shaterabadi et al., 2020; Shaterabadi and Jirdehi, 2020) tried to investigate more about integrating Invelox with other energy production systems, such as photovoltaic panels. Gavade (Gavade et al., 2018) presented a novel idea for capturing wind power to generate electricity more affordably. They reported that the wind speed rose twice at the designed venturi and 6 m/s in the entrance area. Scientists worldwide have identified concepts (Allaei, 2012; Allaei et al., 2015; Al-Bahadly and Petersen, 2011; Bontempo and Manna, 2020; Saeed and Kim, 2017) that indicate customized applications for wind energy production; for instance, the Air Born concept was developed to capture high-speed wind from 300–500 m altitude. Several duct-mounted wind turbines with single and multi-channel varieties are established (Al-Bahadly and Petersen, 2011; Saeed and Kim, 2017; Hosseini and Ganji, 2020a; Bontempo and Manna, 2016). Also, some concepts for shrouded wind turbines require more investigation; however, in some cases, (Visser, 2024) they spend more than 8 years developing their prototype.

On the one hand, ducts are designed in various shapes, including wing, ring-shaped, Invelox, convergent-divergent, and others (Agha et al., 2018; Rahmatian et al., 2023a). On the other hand, most conventional, ducted, air-born, and Invelox wind turbines employ a three-blade rotor connected to a hub at the top of a structure (Taghinezhad et al., 2021a, 2019). Multiple investigations have already been conducted to enhance the outcomes of single-rotor wind turbines, studying the blades' structure and expanding rotor and tower diameter and height to reach more powerful wind speeds at more significant elevations (Teng et al., 2023; Zhou et al., 2023). Large rotors can face various challenges, including pressure distribution along the blade surface, dynamic stress loads, acoustic emissions driven by gravitational stresses and aerodynamic forces, and the need for plenty of space and strong winds for proper functioning (Peng et al., 2023).

Researchers suggested the multirotor idea to enhance the power generated by wind turbines operating within the same sweeping area while supplying affordable energy costs (Mohamed et al., 2019a; Ohya et al., 2017). For instance, in dual rotor turbines, the power-extracting ability for a given swept area is increased by aligning two propellers in a sequence and back-to-back. By comparing multi-rotor (Yuji and Koichi, 2019) and multi-blade (Wang et al., 2013) turbines with single-rotor using experimental and numerical methodologies, several studies have shown that their developed wind turbine can capture wind energy more than conventional generators.

Although the idea of a multi-rotor wind turbine has become less popular, the concept of a multi-rotor wind turbine has experienced a decline in favor owing to the belief that it is complicated; numerous researchers are actively working toward developing multi-rotor wind turbines. According to Khalefa, (Khalefa et al., 2020) the most significant relationship between output power and wind speed determines a wind turbine's efficiency. Since ducted wind turbines are designed to increase the velocity of the wind, using multi-rotors in the ducts provides a new concept to improve their efficiency. Allaei [33] reported a noticeable increase in power rating as an array of propellers was installed in their Invelox. Furthermore, empirical investigations indicate that combining two or three turbines in a convergent-divergent duct for wind turbine setup can outperform a single turbine configuration, achieving 52 % and 72 % efficiency gains, respectively. Despite their experimental study, several data are missing in their reports. For instance, the dimension of the throat section and its specification were not mentioned, making it impossible to compare with future studies. Also, their study did not mention the exact location of the rotors and the distance between them. Mohamed (Mohamed et al., 2019a, 2019b) investigated a two-rotor wind turbine with a lens and reported that the C_p could reach more than 1.0 for the equivalent entering airflow in a low wind velocity zone compared to a single-rotor turbine. Their study used CFD analysis using a third generator, and experimental analysis was not included in their research scope. In the current study, we tried to include all the required information to design a multi-rotor wind turbine to mount in a duct. All parameters are described and expanded for further studies to define comprehensive evaluation criteria for the experimental testing of ducted wind turbines. Also, a wide range of wind speeds was used to discover wind speed's effect on various arrangements of multi-rotor wind turbines.

The previous technique may require considerable time and make it hard to find the ideal situation since there are several interactions. The traditional method might result in uncertainty, inaccurate outcomes, and lengthy processes. Furthermore, it cannot recognize the interactions between two or more variables and fails to provide the ideal situations. A 3D Responsive Surface, as a statistical technique, is a valuable tool for analyzing variables by requiring only a tiny amount of examinations for multiple factors and various variables (Walia et al., 2015). It is frequently employed in multi-level optimization algorithms, optimal condition assessments, and connectivity analysis because it can efficiently evaluate the impact and interactions of numerous factors across various levels. Compared to traditional procedures, this approach requires fewer treatments and less time to achieve optimum efficiency and dependability of test accuracy; (Srivastava et al., 2017) it is frequently employed for developing wind energy technologies, including wind energy recovery in the wake of turbines, (Tabatabaeikia et al., 2016) the efficiency of Invelox diffusers, (Hosseini and Ganji, 2020b) The configurations of the controls of an adjustable-rate wind turbine's frequency adapter (Hasanien and Muyeen, 2012).

So far, no investigation utilizing the 3D surface technique has been conducted on duct-mounted turbines to consider the three-rotor interaction effect, including rotor size and their rotating direction, on generated power. The presented study aims to investigate several factors that affect the output of duct-mounted turbines. Parameters for the duct and impellers are described in detail to be available for other research to conduct in future studies. Rotors were fixed in the pre-designed part of a duct to test the concept that the number, size, and rotating direction of rotors significantly affect the efficiency of ducted wind turbines. This study's primary objective was to design, create, and examine 10 different kinds of multirotor wind turbines that would be installed in a pre-fabricated duct. After designing and fabricating the propeller blades and rotors, the turbines are mounted within the duct's throat. A laboratory assessment of each type of turbine performance inside the duct was conducted. The main objective of this study was to identify which multirotor wind turbine could operate most effectively within a duct. The introduced equipment can be used as an individual system to produce power from wind flow or as the heart of the power-producing setup in some recently developed wind turbine structures such as Airborn and

Invelox.

Compared to previous studies such as Allaei et al. (2015) and Mohamed et al. (2019a, 2019b). explored ducted multi-rotor turbines, their studies lacked precise data on rotor spacing, wake interactions, and power extraction efficiency. The current study provides a detailed experimental assessment, quantifying power output variations across ten multi-rotor configurations. Unlike conventional parametric studies, (Taghinezhad et al., 2019; Mohamed et al., 2019a) which relied on limited experimental setups, we applied a 3D response surface methodology to analyze the interaction of rotor size, spacing, and rotational direction, offering a systematic optimization approach for power efficiency. Compared to the 52 % and 72 % efficiency gains reported by Allaei et al. (2015)). for dual and triple rotors, respectively, our findings indicate that a counter-rotating three-rotor setup (CR-BSB) enhances power efficiency by up to 95 % at high wind speeds (16 m/s). This significantly surpasses previous performance benchmarks. Previous studies often focused on a narrow range of wind speeds (typically 4–12 m/s) (Allaei et al., 2015; Taghinezhad et al., 2019; Mohamed et al., 2019a). Our work examines wind speeds from 4 to 16 m/s, allowing for a more comprehensive understanding of how rotor arrangements respond under various conditions. Many earlier studies focused on numerical simulations, (Mohamed et al., 2019a, 2019b) whereas this research provides experimental validation with precisely defined rotor configurations and duct specifications, making it a valuable reference for future real-world applications. This study bridges gaps in the existing literature and lays the foundation for designing high-efficiency ducted multi-rotor wind turbines tailored to specific wind conditions.

2. Material and methods

2.1. Specification for blade profiles

Identifying a proper blade shape with the best aerodynamic performance is the first step in designing a wind turbine blade for a duct-mounted turbine. Furthermore, the turbines' compact size necessitates that the blades be strong enough to withstand powerful winds. Consequently, NACA 4424 airfoil has been employed to get the blades ready to use (Wern, 2016). The NACA 4424 airfoil was selected for the rotors due to its high lift-to-drag ratio, making it suitable for compact rotor designs where efficient power extraction at low to medium wind speeds is critical. Its symmetrical profile offers stable aerodynamic performance across various angles of attack, which is advantageous for ducted turbine configurations. A conventional type wind generator with three blades and 0.15 m rotor diameter for the big rotors and 0.075 m rotor diameter for the smaller turbines had been proposed for laboratory evaluations, and the blades, hub, and other components of the setup were fabricated based on the duct throat section characterization and turbines setup position. Fig. 1 (A) presents the airfoil's chord length, while the applied pitch angle to the blades is shown in Fig. 1 (B). The chord length has an upper bound value of 20 mm along the blades and around 5 mm at the blade tip.

Fig. 2 displays the simulated blade in Siemens NX PLM CAD and CAM software. Accurate data about blade details are available in a previous study (Taghinezhad et al., 2021a). This data can be utilized to determine the whole blade configuration. The blades were fabricated with a mounting block that enabled them to be attached to the hub through a stereolithography apparatus (SLA) with a resin substance matching the BEM structure.

2.2. Rotors arrangement specification

Independent and dependent factors are considered to examine how the arrangement of the rotors affects the total power of a combined turbine. As an independent variable, the enhanced airflow velocity through the duct was recorded in seven levels of 4, 6, 8, 10, 12, 14, and 16 m/s to cover low, medium, and high-rate ranges. The dependent variables are the shaft's rotational speed and the power generated by the first, second, and/or third rotors. Table 1 outlines the specifications of the rotors utilized in the experimental assessments. As indicated in Fig. 3, the smaller rotor on the compound of rotors has a diameter of 75 mm, while the big rotors have a diameter of 150 mm. Distance between rotors is selected based on, (Taghinezhad et al., 2021a) while D_t is the throat section diameter. The rotors can rotate clockwise and counterclockwise. Ten different configurations were considered for installation in a duct's throat section located in the wind tunnel's test section. Six configs with two rotors were considered for turbine combination, and four others were defined for three-rotor turbines. A rigid shaft connected each rotor to a DC generator in each compound of turbines.

Turbine arrangements which are used in this study are shown in Table 2. The type of rotors and their rotation direction are defined.

Based on the techniques researchers have used to create various wind tunnel sections, the developed and constructed duct by (Taghinezhad et al., 2021b) was utilized in this study. Fig. 4 represents the duct framework, constructed in three parts for duct-mounted turbine setups. The intake component was fabricated using the method that Morel provided (Shi et al., 2021; Zanoun, 2018). The primary position of the turbines was the middle component between the convergent and

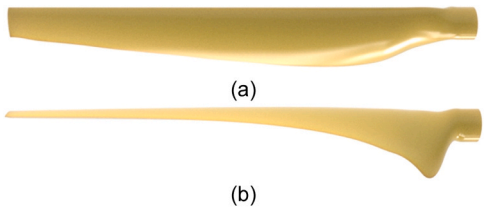

Fig. 2. Fabricated blades front (a) and top (b) perspectives.

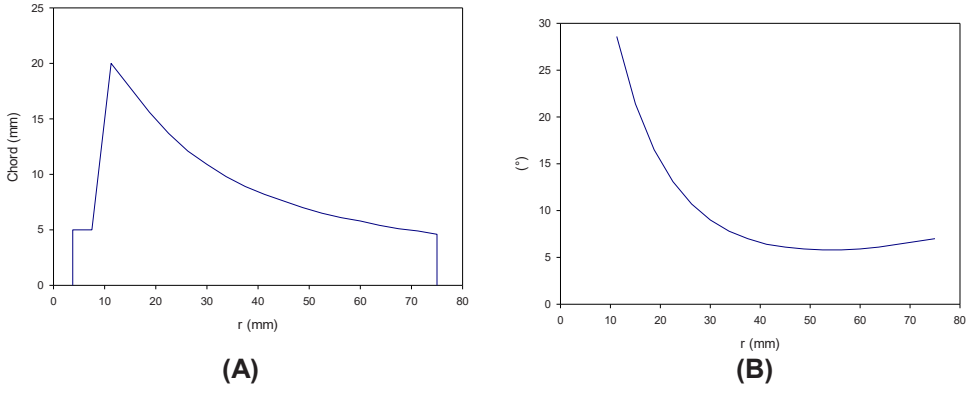

Fig. 1. A diagram showing the chord length of the blade concerning the blade's length (A), Applied pitch angle across the blade (B).

Table 1
Parameters of the rotors employed in this study to make multirotor turbines.

Specification	Big Rotor	Small Rotor
Blade Quantity	3	3
Rotor Sweep Span	150 mm	75 mm
Design Solution	Upwind	Upwind
Blade Profile	NACA 4424	NACA 4424
Blade composition	ABS	ABS
Rotating direction	Clockwise/Counter	Clockwise/Counter

divergent sections of the duct. The divergent discharge component is proposed to release flow and recover the remaining flow impact from the turbines. As this model design aimed to conduct wind tunnel experimental tests, several characteristics of industrial turbines, including a yaw support bearing and weather-resistant components, were ineffective and left out. The duct, shown in Fig. 4, was constructed using ABS polymer and polyurethane coating to provide a completely smooth, finished layer.

2.3. Examination method

The open-circuit wind tunnel in the Faculty of New Sciences and Technologies' Experimental Aerodynamics Lab was used for all the research lab tests at the University of Tehran. We calibrated the wind tunnel's flow stream speed using the pitot technique. Fig. 4 depicts the arrangement of the experimental study. To be calibrated by the wind tunnel's airflow, a hot-wire anemometer probe was initially positioned in the middle point of the test chamber of the wind tunnel. The proposed setup, including the duct and multi-rotor turbine, was mounted in the chamber test, with the validated hot-wire sensor attached to the duct's throat to detect the wind velocity online. The most significant wind velocity it can achieve in the Atmospheric Boundary Layer (ABL) is 45 m/s. The specifications for the suction-based wind tunnel are a horizontal fan, a diffuser, a testing location, a nozzle, a bell-curved intake, and an expansion chamber with multiple mesh screens. An exterior glimpse of the wind tunnel setup, including the flow suction fan, is shown in Fig. 4The uniformity of the wind was unable to be tracked. The test part is 1.5 m long, while the tunnel structure is 12.5 m long. Additionally, the test part is one meter wide and 0.7 m tall. The wind tunnel's test area normal-level turbulence intensity was computed to be 0.4 %.

A fan with 6000 hp power provided independent control of the flow stream's wind velocity. A portable anemometer with one probe recorded the wind velocity. It demonstrates an average fluctuation of ±1 % in the fluid flowing to the mounted turbine. It was found that the flow field turbulent movements varied by 5–10 % across the entire range of entrance wind velocity. The blockage ratio of the developed setup was checked in the test area and found to be 11.4 %. The blockage did not affect the test outcomes [25]. The setup was examined in an open-duct configuration without any rotating turbine. The rotor was mounted to the duct setup, and further runs were conducted after gathering a suitable amount of data through multiple runs. The generated voltage and measured current for generators were recorded throughout the evaluation process. The obtained data was subsequently submitted to a computing device for processing and evaluation. By multiplying the reported current (I_L) by each rotor's output voltage (V_T), we can determine the level of extracted power provided by the DC generators (Pape and Kazerani, 2020). The sum of the produced power by all the mounted rotors in the duct throat was considered the total output power for each combination of rotors, Eq.1.

$$P_{total} = \sum I_L \times V_T \quad (1)$$

To conduct the tests, 10 different configurations of wind turbines were installed inside a prefabricated duct. The turbines were tested in three ranges of wind speed, Low Wind Speeds (4–6 m/s), Medium Wind Speeds (8–12 m/s), and High Wind Speeds (14–16 m/s) to evaluate their power performance in different conditions. A 3D response surface methodology (RSM) was used to analyze the interaction between rotor size, spacing, and rotational direction. This statistical technique allowed for the optimization of rotor configurations with fewer experimental trials than traditional methods.

3. Results and discussion

3.1. Generated power equality

To ensure that all generators produce the same amount of electricity under the same input, load, and environmental circumstances, all three turbines were tested according to the method introduced by 28.33. The

Table 2
Turbine details and characterization.

Turbine Configuration	1st Rotor	2nd rotor	3rd Rotor	Rotation Status
BBB-CO	Big	Big	Big	CO
BSB-CO	Big	Small	Big	CO
BBB-CO	Big	Big	Big	CO
BSB-CR	Big	Small	Big	CR
BS-CO	Big	Big	-	CO
SB-CO	Small	Big	-	CO
BB-CO	Big	Big	-	CO
SB-CR	Small	Big	-	CR
BS-CR	Big	Small	-	CR
BB-CR	Big	Big	-	CR
BB-CR	Big	Big	-	CR
Single	Big	-	-	-

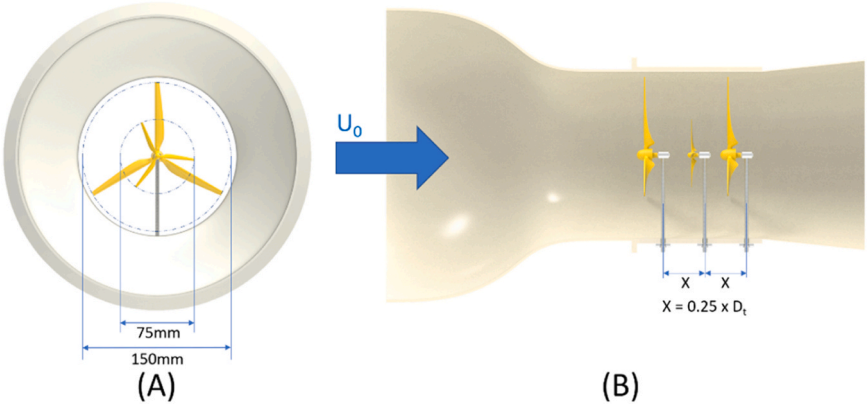

Fig. 3. Rotors are mounted within the duct front view (A) and section view (B), and variables are set as shown.

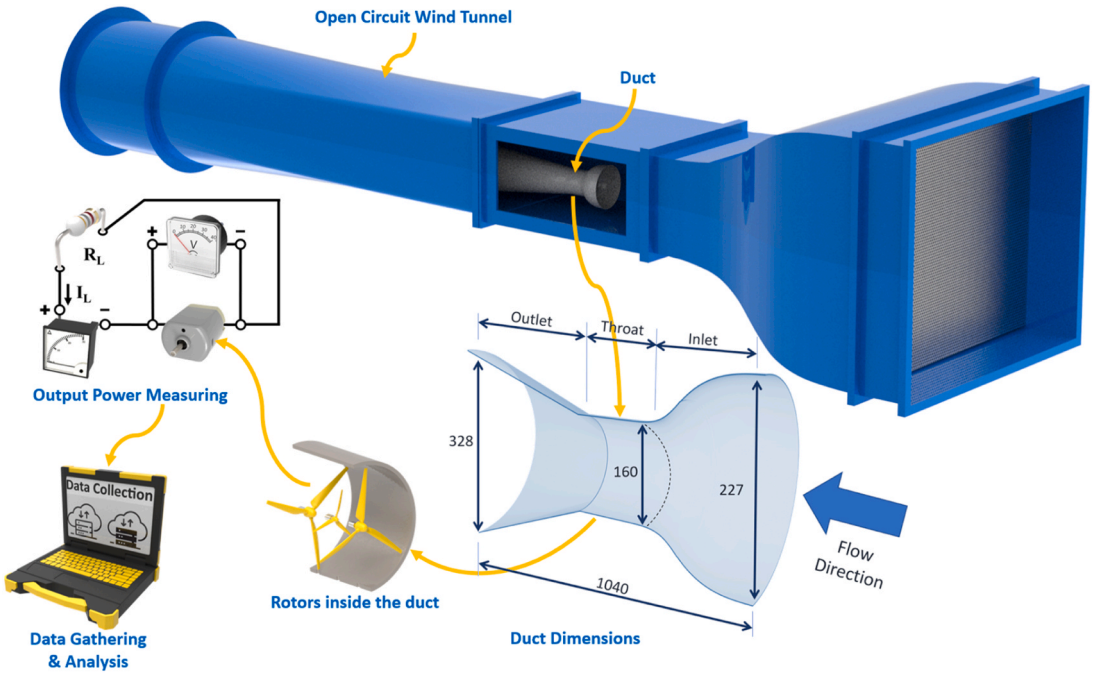

Fig. 4. Configuration of the testing procedure for evaluating the generated power.

output of each DC motor was the same. Fig. 5 shows the output voltage and generated power for utilized DC generators independently, as determined by the turbine spin rate. To confirm similar output, the generators were tested under equivalent environmental conditions, such as wind load and intake wind velocity. At around 3800 rpm, the maximum output power that could be achieved was 2.1 W, and the maximum voltage achieved was 270 mV. The DC generators in this study can be replaced with each other in a multi-rotor arrangement, as the voltage and power outputs for both generators are the same.

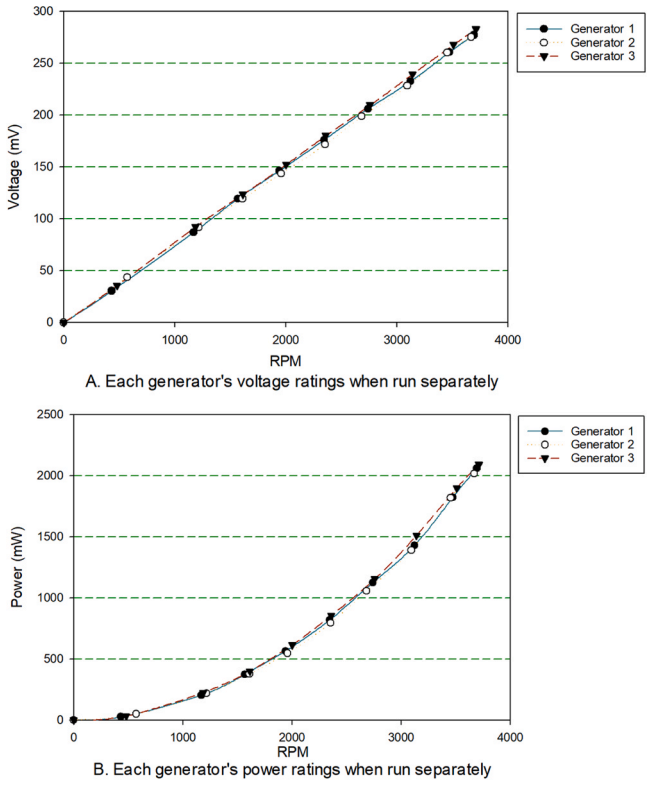

Fig. 5. Generators output voltage (A) and their generated power (B) in a controlled situation.

3.2. Evaluation of multi-rotor turbines generated power

The consideration became provided for using two or three rotors in a duct throat and the impact of the turbine rotating pattern on the amount of generated power. Abbreviations are utilized in the rotor labels and configurations to make them simpler. Letters S and B represented small and large rotors, respectively. For instance, when referring to the first upwind rotors for a set of turbines, the BS sets up a large rotor in the leading position and a small blade rotor at the back. This process proceeds from the left side. Additionally, the co-rotating turbine rotation was identified by the code "CO" and the counter-rotating rotation by the code "CR". A classic instance of a Three-rotor generator is the BSB-CR, which has a counter-rotating small rotor at the midpoint of two big rotors.

3.2.1. Evaluation and comparison of two and three rotors ducted wind turbines

To make a sensible comparison among single, double, and triple rotor installations in ducted wind turbines, we consider ten different arrangements, half operating in a similar direction while the others were rotating in counter mode. The rotors were tested in three levels of high (14 m/s), mid-range (10 m/s) and low (6 m/s) wind velocity, and the outcomes are illustrated in Figs. 6–8, respectively. By analyzing Fig. 6It is estimated that counter-rotating wind turbines perform better at high-velocity winds than co-rotating turbines; BSB, BBB, and SB counter-rotating generators with almost 1.88, 1.84, and 1.76 power ratios were the top performers at high wind velocity. The interaction of the counter-rotating rotors' wakes causes a more uniform wind flow over the second and third turbine blades. This arrangement can mitigate the flow turbulence, which leads to overall performance increases.

However, counter-rotating wind turbines perform better at midrange wind velocity (Fig. 7); three big rotors performed better when a smaller rotor was mounted in the middle of two big rotors. The BBB rotor output power ratio increased by almost 3 %, while the BSB rotor performance was reduced by about 14 % by decreasing airflow velocity from 14 m/s to 10 m/s. It shows that installing a small wind turbine between two big

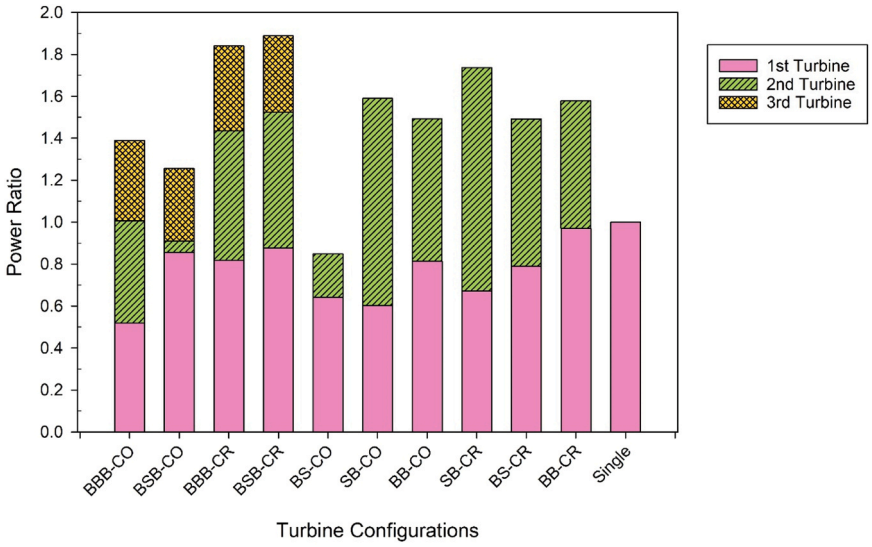

Fig. 6. Comparison of measured power ratio for two and three rotor arrangements at 14 m/s airflow.

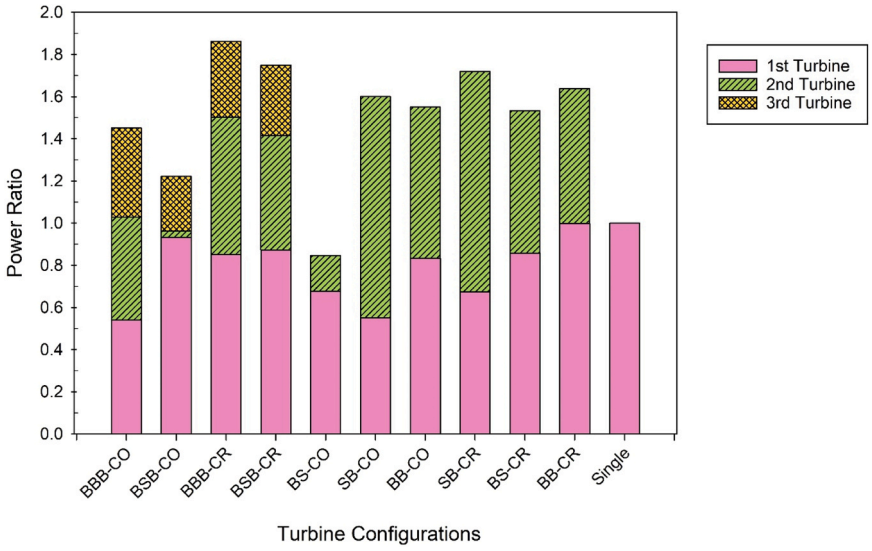

Fig. 7. Comparison of measured power ratio for two-rotor and three-rotor wind turbines at 10 m/s airflow.

rotors can improve the total output power of ducted wind turbines. There are two reasons for this situation: First, more flow can go through the throat section by reducing the resistance to inlet flow at the high-speed wind. Second, installing a small turbine can improve the flow quality at the wake of the first rotor, reduce the interaction among turbines, and extract more output power.

The last comparison for all ten types of turbines for low-speed wind turbines is shown in Fig. 8. Three big counter-rotating rotors show the highest power ratio with a rate of 2.11 compared to the single big rotor, three big co-rotating rotors, and two big counter-rotating rotors with almost 1.79 and 1.7 power ratios were the following high-performance rotors. Due to a cut in speed and small blades, small wind turbines cannot operate at the behind of big rotors at this wind speed. Then, rotors with a combination of big and small rotors do not have an acceptable output compared to big rotors.

3.3. *Effect of installing three rotors at the throat section*

We investigated their performance in a separate section to better compare three-rotor wind turbines. The total extracted power for four different arrangements of generators at various wind velocities is shown in Fig. 9. The effect of installing a small rotor in both the same and opposite-rotating conditions in the middle of two oversized rotors was investigated. In the low-speed winds, the output seems similar for different arrangements. At the same time, for speeds higher than 10 m/s, counter-rotating generators show a higher power output than co-rotating wind turbines. By considering the single-rotor generator as a reference for comparison between arrangements, the rate of extracted power for each type of arrangement is estimated for each wind velocity and is shown in Fig. 10. It is shown that three oversized counter rotors show stable output power in all wind speeds as the output rate in all speeds does not reduce to lower than 1.81 rates of single rotor generator. While for wind speeds above 12 m/s, installing a small rotor in the middle of two big rotors shows a higher output, at the end of the trend (16 m/s), it reaches the power ratio of 1.95. By comparing three big counter-rotating rotors with a small rotor counter rotor at the midpoint, it was found that by replacing a small rotor for wind speeds 12, 14, and 16 m/s, we extracted 5, 6, and 11 percent more power. On the other hand, the highest power ratio occurred for three big rotors at 6 m/s wind velocity, with a rate of 2.11 compared to a single generator.

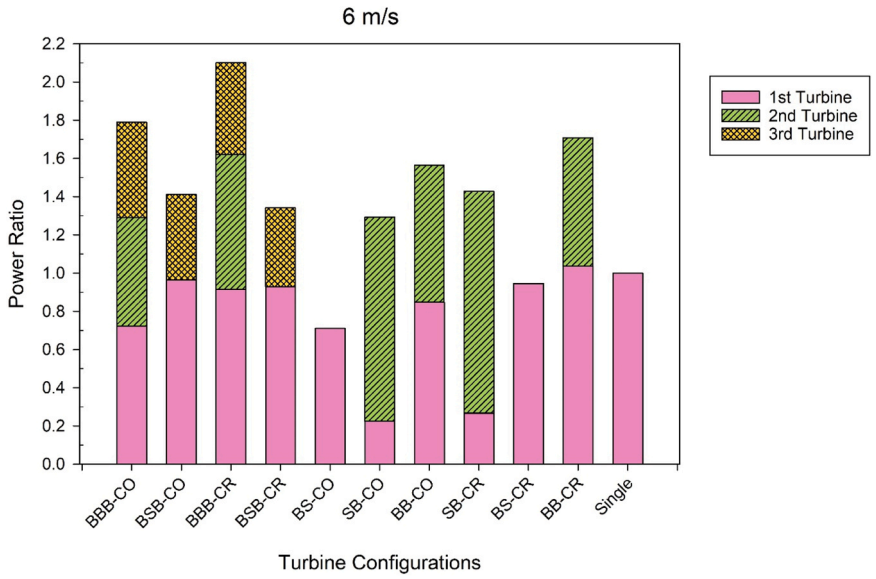

Fig. 8. Comparison of measured power ratio for two-rotor and three-rotor wind turbines at 6 m/s airflow.

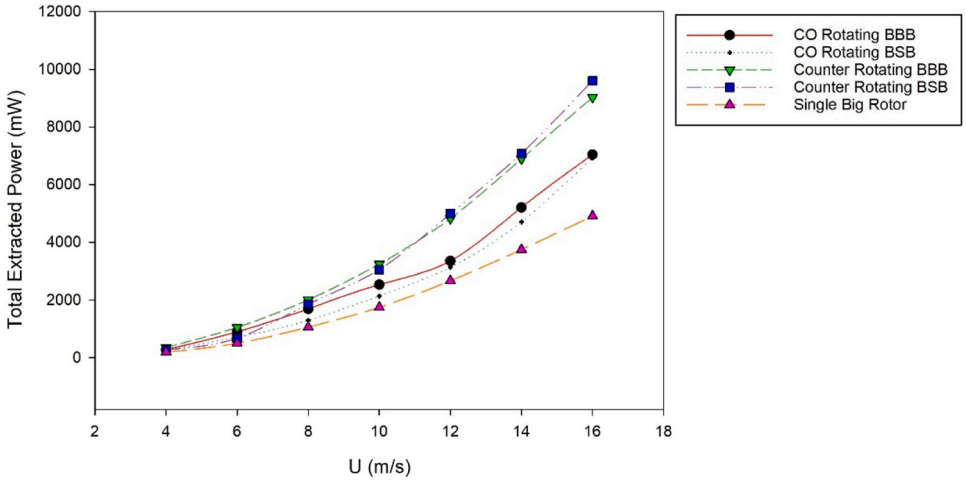

Fig. 9. Total power (mW) extracted from three generators installed in the throat section compared to a single generator.

3.4. Sensitivity analysis

The sensitivity analysis evaluates the rate of change in power ratio concerning wind speed variations for different turbine configurations. This helps in assessing the robustness of each setup under varying wind conditions. Single Big Rotor served as a baseline for comparison. For the CO-BBB configuration, the highest sensitivity is observed in the low-to-mid wind speed range (4–8 m/s), with values decreasing as wind speed increases. The sensitivity values fluctuate, indicating that this configuration is affected by changes in wind speed but lacks a consistent trend. At higher wind speeds (10–16 m/s), sensitivity decreases, suggesting a potential saturation effect where further wind speed increases yield diminishing returns in power output. CR-BBB configuration exhibits a relatively high sensitivity at lower wind speeds, peaking around **6–8 m/s** before stabilizing. Compared to CO-BBB, this configuration maintains a more consistent power ratio increase across wind speeds. The lower variability suggests improved performance robustness under varying wind conditions. CO-BSB displays negative sensitivity values in some regions (6–8 m/s), indicating a drop in power ratio with increasing wind speed. This suggests that aerodynamic losses or inefficiencies may reduce the overall power gain at certain wind speeds. However, at higher wind speeds (12–16 m/s), sensitivity becomes positive, showing improved performance. CR-BSB configuration shows a gradual and stable increase in sensitivity with wind speed. Unlike CO-BSB, this configuration maintains a positive sensitivity across all wind speeds, highlighting better adaptability to wind variations. The relatively high sensitivity at higher wind speeds suggests it benefits more from increasing wind velocity than other configurations. Sensitivity analysis shows that CR-BBB and CR-BSB configurations demonstrate the most consistent and favorable sensitivity trends, making them more robust for real-world applications. Therefore, we conducted an intensive study on these two configurations in the next section.

3.5. Analyzing of rotors interaction for counter-rotating BBB and BSB turbines

To investigate more details about the performance of three big counter-rotating generators (Fig. 11) and compare it with a replaced small rotor in the midpoint (Fig. 12), we fit a 3-D surface to the extracted data to find the interaction of rotors and their effect on the extracted power ratio in both compounds of rotors. In Fig. 11 (A–C), the interaction of the output power ratio of each generator versus the total outpour

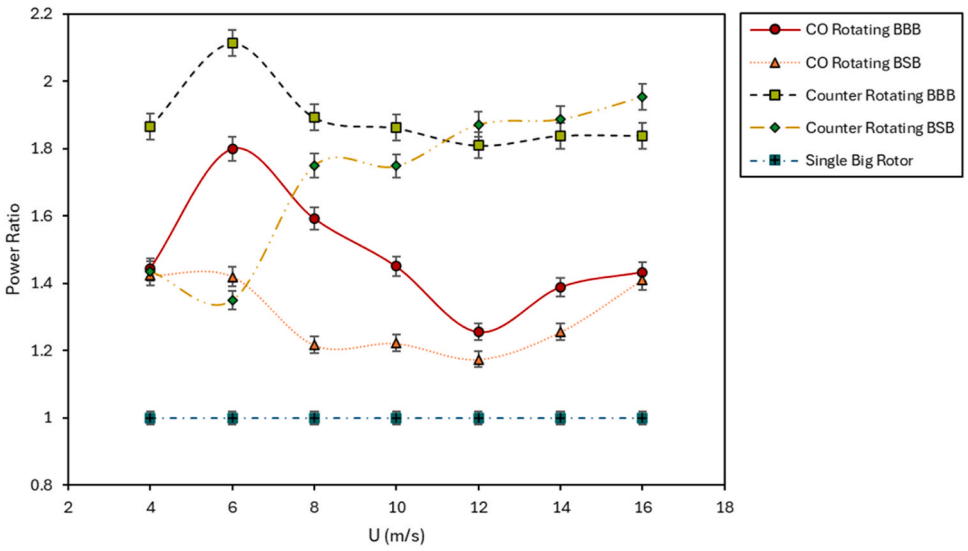

Fig. 10. Extracted power ratio for mixed three generators in comparison to single rotor.

power ratio is shown. The interaction between G1 and G2 in Fig. 11 (A) revealed that the second generator is more sensitive to the output power ratio than G1. Also, from Fig. 11 (D and E), it is estimated that the highest output for the G1 power ratio occurred in low-speed wind turbines. However, the range of suitable outcomes for G2 was wider, and the best output was reported in the low-speed winds.

The interaction between G1 and G3 in Fig. 11(B) shows a hyperbolic parabola relationship between the two generators. Fig. 11(D and F) reveals that the highest total power ratio occurs in low-speed winds for G1 and G3. As the speed increases to 16 m/s, the total extracted power is reduced by about 30 % in the worst case. On the other hand, from Fig. 11 (B), the highest output power was reported in the lower outcome of generators 1 and 3; from this analysis, it can be concluded that in lower wind speeds, better performance is possible for the compound of turbines. Also, it is shown that if we focus on improving the performance of only one of the generators, its effect on the two other generators will

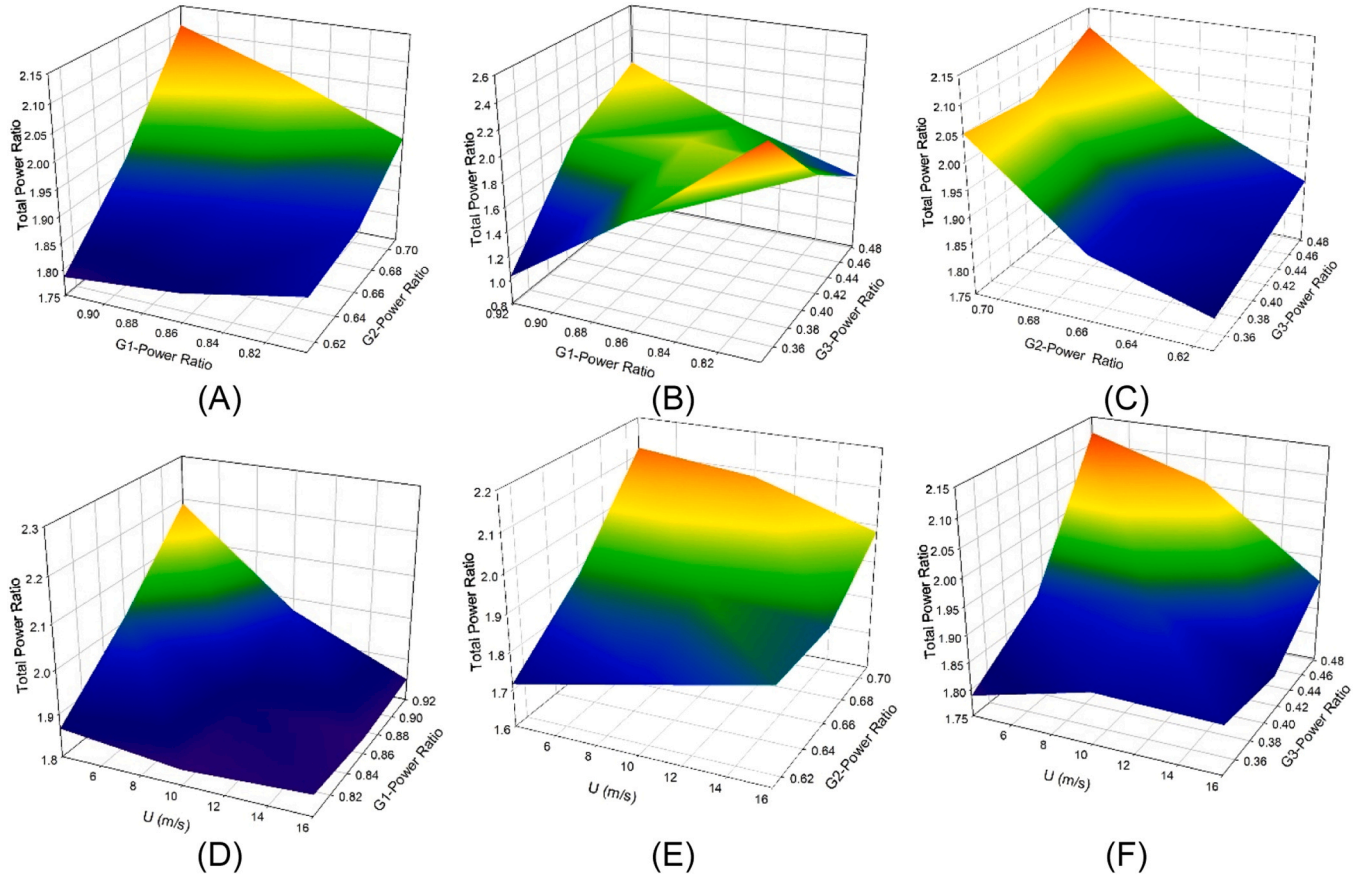

Fig. 11. Investigation of the interaction of factors for Three big counter-rotating generators for the power ratio in Generators 1 & 2 (A), 1 & 3 (B), and 2 & 3 (C), also wind speed and each generator power ratio on total extracted power for G1 (D), G2 (E), and G3 (F).

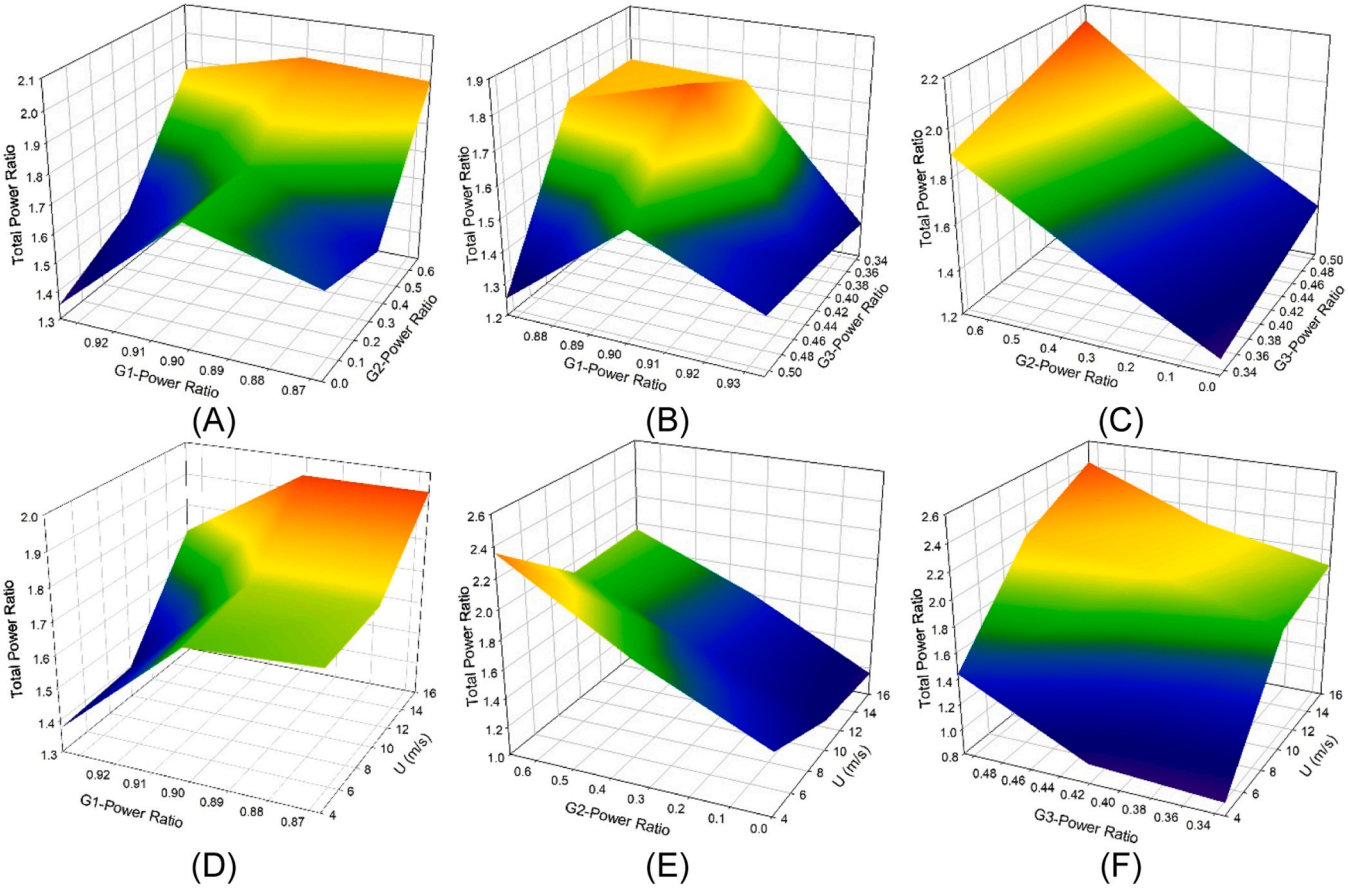

Fig. 12. Investigation of the interaction of factors for three counter-rotating generators with a smaller one in the midpoint for the output power rate in Generators 1 & 2 (A), 1 & 3 (B), and 2 & 3 (C), also wind speed and each generator power ratio on total extracted power for G1 (D), G2 (E), and G3 (F).

show a significant reduction in the rate of total output power. The interaction between G2 and G3 and their response to total extracted power at different wind speeds is shown in Fig. 11(C, E, and F). It can be seen that G2 is more sensitive than G3, and positive change in G2 causes a better performance in G3. In the same way, both generators show their best output rate at the lowest wind speed. Overall, from the analysis of Fig. 11, it is demonstrated that G2 has a sensitive role in total output power, and by improving its efficiency, it is possible to optimize the amount of power rate extraction in two other generators. Generators G1 and G3 show a parabolic relation on total extracted power, so we cannot focus only on optimizing one to find a better output rate. The most restrictive rule among all generators is that when they are working in a complex of three big counter-rotating arrangements, the highest performance for all generators can be reached at the lowest speeds of wind, for instance, at 4 m/s airflow, the highest rate of change in output power rate with almost 12 %, 8 %, and 13 % excess for G1, G2, and G3 is possible, respectively.

Fig. 12(A–C) shows the interaction of generators' output power ratios on the total output power ratio when a small counter-rotating rotor is replaced at the midpoint of two big rotors. Considering Fig. 12(A) for G1 and G2 interaction, the total output ratio is estimated to be more sensitive to the G2 power ratio. At the same time, from Fig. 12(D-E), it is reported that G2 is reacting quicker to the changes in wind speed. As the airflow velocity increases, the power extraction in G2 is increased. In this situation, more output power can be reached. On the other hand, from G1 in Fig. 12(D), It is apparent that the highest total output power ratio was achieved when around 90 % of energy was harvested in G1. The interaction between G1 and G3 is presented in Fig. 12(B). From Fig. 12(F), it is clear that the changes in G3 are not so sensitive to the wind speed compared to G1 and G2. Also, in contrast with the two other generators, the output rate in G3 increased by enhancing the wind speed, and the highest output occurred when this turbine's production reached its maximum value. By exploring the interaction between G1 and G3, we found that the optimum condition for maximizing the output can be reached at around 90 % for G1 and 0.42 for G3. The interaction between G2 and G3 is shown in Fig. 12(C), where perturbation analysis shows that G2 affects the total power ratio more. Also, by increasing the extracted power from each generator, the rate of total power increased significantly.

Fig. 13 shows the measured values for three big counter-rotating (A) and two big ones with a small rotor at the midpoint (B). As the only change is that a small opposite spinning rotor is installed at the midpoint of two big generators, it is possible to investigate the effect of this change on other generators compared to three counter-rotating big generators. In low-speed winds (4 and 6 m/s), the small rotor does not work due to its higher cut-in speed. This causes the third Generator, G3, to extract more power ratio than the other turbine (A), reaching a 51 % power rate at 4 m/s. However, the rate for G1 shows more value in the BSB compared to the CR-BBB turbine; the reported total output power for BBB is almost 40 % higher than the BSB counter-rotating. It reveals the effect of cut-in speed on output power, where lower cut-in speed for big rotors caused a higher outcome in low airflow velocities; for instance, 4 m/s, the second big rotor at BBB arrangement enhanced the total output power by about 40 % in comparison to BSB and reached to a peak of 70 % at 6 m/s. At 8 m/s of wind speed, the 2nd small generator contributes to power extraction, and it can raise the total power ratio to almost 40 % compared to 6 m/s wind speed. However, the rate for CR-BBB remained stable at 10–16 m/s wind speeds; for CR-BSB, the rate rose as the wind speed increased, reaching 1.89 and 1.95 at 14 and 16 m/s wind speeds, respectively. These results prove that CR-BSB wind

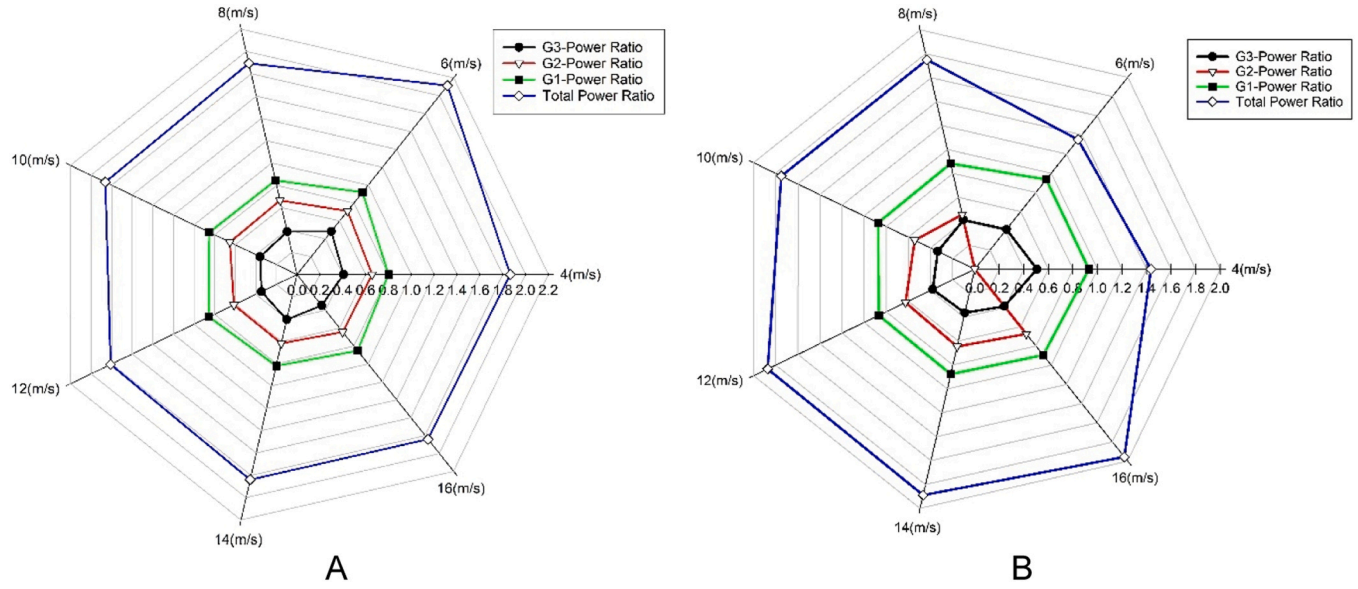

Fig. 13. Comparison between three big counter-rotating generators (A) and replacing a small rotor at the midpoint (B).

turbines have the best performance in wind speeds higher than 14 m/s, while CR-BBB arrangements have a better performance in wind speed from 4 to 12 m/s. It is important to note that these values for wind speed are reported for ducted wind turbines. Then, we should consider the rate of wind speed enhancement caused by the duct to consider suitable conditions for selecting the best arrangement for wind turbines. For instance, according to, (Taghinezhad et al., 2024) the duct used in this study can enhance the wind speed to 2.9 times that of the free stream. Then, in regions with 5.5 m/s wind speed, we can reach 16 m/s flow speed at the throat section.

The optimum conditions to reach the maximum output power at different wind speed levels are reported in Table 3.

In this study, multi-rotor wind turbines with different kinds of rotor arrangements were tested. The comparisons between investigated factors and responses and those from earlier studies are shown in Table 4. This study's reported power ratio for multi-rotor arranged turbines exceeded that of earlier studies. This research demonstrates that, in addition to the duct impact on generated power, the number and direction of rotors in duct-mounted multi-rotor turbines can enhance the extracted power ratio. In contrast, the performance of multi-rotor wind turbines in duct-mounted turbines can be fine-tuned using 3D surface models as an optimization approach because they can identify the impact and interaction of rotors on total output power. Prior studies have identified many techniques to enhance the efficiency of dual or multirotor wind turbines in specific domains. Compared to two- and single-rotor wind turbines, the generated power gained for three-rotor wind turbines was considerably higher. Meanwhile, there is no set approach to examine the efficiency of the various multi-rotor turbine designs located in a duct, so this paper can test and compare multi-rotor wind turbines to expand their use for ducted wind turbines.

Table 3
The best-fitted values for the design variables and outcomes.

Variable	Range	Low Speed	Mid-Speed	High Speed
Airflow Velocity (m/s)	4–16	4–8	8–12	12–16
Space Between Rotors	Throat Diameter	0.25	1.	0.25
Rotors Arrangement	As Described	CR-BBB	CR-BBB	CR-BSB
Max. Power Ratio	Maximum	2.1	1.89	1.95
Speed at Maximum power ratio	In range	6	8	16
Power (mW)	Maximum	1048	2422	9597

4. Conclusion

The aerodynamics of multi-rotor arrangements, which include two or three wind turbines spaced 0.25 of the duct throat diameter in a row and in front of a uniform flow, were investigated in wind tunnel experimental tests. The effect of size and direction rotation of rotors on output power was studied. Most opposite-spinning multi-rotor turbines are advantageous against same-direction-rotating turbines as they generate more power in the same condition. The reported results for 10 models of turbine type at different wind speeds showed that the rotor arrangement significantly affects the generated power. The CR-BBB configuration presented the highest power ratio of 2.1 at low wind speeds (6 m/s), producing 1048 mW. At moderate wind speeds (10–12 m/s), the CR-BBB arrangement maintained a power ratio of 1.89, generating 2422 mW. At high wind speeds (14–16 m/s), the CR-BSB configuration outperformed others, reaching a peak power ratio of 1.95 and generating 9597 mW at 16 m/s - approximately 95 % higher efficiency compared to a single-rotor setup. The interaction of rotors regarding the individually generated power was investigated for CR-BSB and CR-BBB turbines. The optimum condition overview shows that CR-BBB could show the best acceptable power output in all wind speed ranges. In contrast, for the high-range wind velocities, the generated power by CR-BSB rocketed, and in wind speeds of about 16 m/s, it can produce almost 12 % more than CR-BBB. Then, it is worth studying the wind maps of zones where you want to install a ducted wind turbine, and considering that the right arrangement can show a valuable increase in output power. The result of this article is a complete guide on selecting a suitable arrangement of wind turbines based on the prevailing wind in the area and the wind expansion ratio in the designed duct. For instance, by finding 6 m/s as the most delivered wind speed to mounted turbines in the duct throat section, you can select CR-BBB by a generated power ratio of 2.1 times compared to a single rotor. The presented study is beneficial in finding the optimized extracted power of multi-rotor wind turbines to meet specific experimental objectives. Then, the complexity of doing repeated practical trials and the associated expenses are minimized, and quick decision-making is created for developing multi-rotor applications in ducted wind turbines. In addition to lowering costs, standardization in production might also be beneficial for desired-size rotors used in multi-rotor systems. While this study provides a detailed experimental assessment of ducted multi-rotor wind turbines,

Table 4
A comparison of the current project's findings with those of earlier research.

No.	References	Optimum Parameters			Enhanced Output Ratio
		Airflow Velocity (m/s)	Space Between Rotors	Rotor Arrangement	
1	(Shen et al., 2007)	5–20	0.1–0.8 Turbine Radius	CR-BB	43.5 %
2	(Allaei et al., 2015)	4–12	N/A	CO-BB	52 %
3	(Allaei et al., 2015)	4–12	N/A	CO-BBB	72 %
4	(Agung Bramantya et al., 2016)	4.2	0.44 Turbine Radius	CR-SB	24 %
5	(Wang et al., 2018)	6.5	0.25 Throat Diameter	CR-SB, CO-SB	7.2 %
6	(Didane et al., 2018)	5	0.16 m	CR-BB	40 %
7	(Taghinezhad et al., 2021a)	20	0.25 Throat Diameter	CR-BB	55 %
8	(Rahmatian et al., 2023b)	5–7.1	0.2–0.6 m	CO-BB CO-SB	23 %
9	Current Study	4–12	0.25 Throat Diameter	CR-BBB	110 %
10	Current Study	14–16	0.25 Throat Diameter	CR-BSB	95 %

future research can explore additional factors to enhance efficiency and real-world applicability. Potential future directions include full-scale testing, advanced aerodynamic modeling, wake interaction studies, and hybrid renewable energy systems integration.

CRediT authorship contribution statement

Javad Taghinezhad: Formal analysis, Validation, Writing – original draft, Methodology, Data curation, Writing – review & editing, Investigation, Software. **Mohammad Omidyeganeh:** Writing – review & editing. **Mehran Masdari:** Investigation, Supervision, Funding acquisition, Data curation, Writing – original draft.

Declaration of Competing Interest

The authors declare that they have no known competing financial interests or personal relationships that could have appeared to influence the work reported in this paper.

Data availability

Data will be made available on request.

References

Agha, A., Chaudhry, H.N., Wang, F., 2018. Diffuser augmented wind turbine (DAWT) technologies: a review. Int. J. Renew. Energy Res. 8, 1369–1385.

Agung Bramantya, M., Huda, L., Al, 2016. An experimental study on the mechanics power of counter rotating wind turbines model related with axial distance between two rotors. 2016 6th International Annual Engineering Seminar (InAES), Yogyakarta, Indonesia CRWT. Yogyakarta, Indonesia, pp. 212–217. https://doi.org/10.1109/INAES.2016.7821936.

Akhtar, N., Geyer, B., Schrum, C., 2024. Larger wind turbines as a solution to reduce environmental impacts. Sci. Rep. 14, 6608.

Akhter, M.Z., Shaaban, A., Marini, A., 2024. Enhancing power output of ducted wind turbines through flow control. J. Phys. Conf. Ser. 2767, 072011.

Al-Bahadly, I., Petersen, A.F.T., 2011. Wind turbines. A Ducted Horizontal Wind Turbine for Efficient Generation. InTech.

Allaei, D. Using CFD to Predict the Performance of Innovative Wind Power Generators. in Proceedings of the 2012 COMSOL Conference in Boston 2–3 (2012). doi:10.1111/1467-9655.12497.

Allaei, D., Andreopoulos, Y., 2013. INVELOX: a new concept in wind energy harvesting. ASME 2013 7th Int. Conf. Energy Sustain. 15.

Allaei, D., Andreopoulos, Y., 2014. INVELOX: description of a new concept in wind power and its performance evaluation. Energy 69, 336–344.

Allaei, D., Tarnowski, D., Andreopoulos, Y., 2015. INVELOX with multiple wind turbine generator systems. Energy 93, 1030–1040.

Amiri, M.M., Shadman, M., Estefen, S.F., 2024. A review of physical and numerical modeling techniques for horizontal-axis wind turbine wakes. Renew. Sustain. Energy Rev. 193, 114279.

Aravindhan, N., et al., 2024. Experimental and numerical analysis of building-mounted INVELOX wind turbines. Iran. J. Sci. Technol. Trans. Mech. Eng. 48, 907–918.

Ayaz, A., Israr, A., Khan, M.Z., 2023. Numerical and experimental investigation of geometric parameters influence on power generation of INVELOX wind turbine. Energy Sustain. Dev. 77, 101329.

Bayati, M., 2024. Design and performance evaluation of a mid-range airborne wind turbine. Arab J. Sci. Eng. 49, 15021–15036.

Bontempo, R., Manna, M., 2016. Effects of the duct thrust on the performance of ducted wind turbines. Energy 99, 274–287.

Bontempo, R., Manna, M., 2020. Diffuser augmented wind turbines: review and assessment of theoretical models. Appl. Energy 280, 115867.

Cao, Y., Su, E., Sun, Y., Wang, Z.L., Cao, L.N.Y., 2024. A rolling-bead triboelectric nanogenerator for harvesting omnidirectional wind-induced energy toward shelter forests monitoring. Small 20.

Didane, D.H., Rosly, N., Zulkafli, M.F., Shamsudin, S.S., 2018. Performance evaluation of a novel vertical axis wind turbine with coaxial contra-rotating concept. Renew. Energy 115, 353–361.

Dou, B., Guala, M., Lei, L., Zeng, P., 2019. Wake model for horizontal-axis wind and hydrokinetic turbines in yawed conditions. Appl. Energy 242, 1383–1395.

Firoozi, A.A., Hejazi, F. & Firoozi, A.A. Advancing Wind Energy Efficiency: A Systematic Review of Aerodynamic Optimization in Wind Turbine Blade Design. Energies (Basel) **17**, 2919 (2024).

Gao, X., Yang, H., Lu, L., 2016. Optimization of wind turbine layout position in a wind farm using a newly-developed two-dimensional wake model. Appl. Energy 174, 192–200.

Gavade, A.A., Mulla, A.S., Ransing, A.M., Sane, N.M., 2018. Design and manufacturing of INVELOX to generate Wind power using nonconventional energy sources. Int. J. Adv. Res. Sci. Eng. 07, 588–592.

Hasanien, H.M., Muyeen, S.M., 2012. Design optimization of controller parameters used in variable speed wind energy conversion system by genetic algorithms. IEEE Trans. Sustain Energy 3, 200–208.

Heidari, R., Ahmadi Jirdehi, M., Shaterabadi, M., 2024. Hybrid energy-based electric vehicles charging station integrated with INVELOX wind turbine: a case study of Kermanshah. Energy 308, 132833.

Hosseini, S.R., Ganji, D.D., 2020a. A novel design of nozzle-diffuser to enhance performance of INVELOX wind turbine. Energy 198, 117082.

Hosseini, S.R., Ganji, D.D., 2020b. A novel design of nozzle-diffuser to enhance performance of INVELOX wind turbine. Energy 198, 1–16.

Hu, W., Yang, Q., Yuan, Z., Yang, F., 2024. Wind farm layout optimization in complex terrain based on CFD and IGA-PSO. Energy 288, 129745.

Khalefa, M.Z., Abd Alkarim, S.F., Salih, R.S., 2020. Optimized Manufacturing of the Small Dual Wind Turbine Used to Generate Electricity in Central Iraq Areas. IOP Conference Series: Materials Science and Engineering, 765. IOP Publishing, pp. 1–15.

Kim, S.-H., Shin, H.-K., Joo, Y.-C., Kim, K.-H., 2015. A study of the wake effects on the wind characteristics and fatigue loads for the turbines in a wind farm. Renew. Energy 74, 536–543.

Li, J., Dao, M.H., Le, Q.T., 2024. Data-driven modal parameterization for robust aerodynamic shape optimization of wind turbine blades. Renew. Energy 224, 120115.

Mangano, M., 2023. High-fidelity. Aerostruct. Des. Optim. Wind Turbine Rotors. https://doi.org/10.7302/22915.

Mohamed, A., El-Baz, A., Abd-Elaziz, N., Mostafa, A., 2019b. Computational investigation of ducted dual rotor wind turbine. NILES 2019 Nov. Intell. Lead. Emerg. Sci. Conf. 29–33. https://doi.org/10.1109/NILES.2019.8909321.

Mohamed, A., El-Baz, A., Mahmoud, N., Hamed, A., El-kohly, A., 2019a. CFD simulation of ducted dual rotor wind turbine for small-scale applications. Proceedings of the GT India. American Society of Mechanical Engineers. https://doi.org/10.1115/GTINDIA2019-2326.

Mozafari, M., Sadeghimalekabadi, M., Fardi, A., Bruecker, C., Masdari, M., 2024. Aeroacoustic investigation of a ducted wind turbine employing bio-inspired airfoil profiles. Phys. Fluids 36.

Ohya, Y., Miyazaki, J., Göltenbott, U., Watanabe, K., 2017. Power augmentation of shrouded wind turbines in a multirotor system. J. Energy Resour. Technol. 139.

Ouyang, K., Chen, T.Y. & You, J.J. Utilizing the Taguchi Method to Optimize Rotor Blade Geometry for Improved Power Output in Ducted Micro Horizontal-Axis Wind Turbines. Sustainability (Switzerland) **16**, (2024).

Pape, M., Kazerani, M., 2020. An offshore wind farm with DC collection system featuring differential power processing. IEEE Trans. Energy Convers. 35, 222–236.

Peng, H., Li, S., Shangguan, L., Fan, Y., Zhang, H., 2023. Analysis of wind turbine equipment failure and intelligent operation and maintenance research. Sustainability 15, 8333.

Qian, X., et al., 2024. Flutter limit optimization of offshore wind turbine blades considering different control and structural parameters. Ocean Eng. 310, 118558.
Qiao, Y., Han, S., Zhang, Y., Liu, Y., Yan, J., 2024. A multivariable wind turbine power curve modeling method considering segment control differences and short-time self-dependence. Renew. Energy 222, 119894.
Rahmatian, M.A., Hashemi Tari, P., Majidi, S., Mojaddam, M., 2023b. Experimental study of the effect of the duct on dual co-axial horizontal axis wind turbines and the effect of rotors diameter ratio and distance on increasing power coefficient. Energy 284, 128664.
Rahmatian, M.A., Nazarian Shahrbabaki, A., Moeini, S.P., 2023a. Single-objective optimization design of convergent-divergent ducts of ducted wind turbine using RSM and GA, to increase power coefficient of a small-scale horizontal axis wind turbine. Energy 269, 126822.
Saeed, M., Kim, M.H., 2017. Aerodynamic performance analysis of an airborne wind turbine system with NREL Phase IV rotor. Energy Convers. Manag 134, 278–289.
Schmidt, H., et al., 2024. How do residents perceive energy-producing kites? Comparing the community acceptance of an airborne wind energy system and a wind farm in Germany. Energy Res. Soc. Sci. 110, 103447.
Shaterabadi, M., Jirdehi, M.A., Amiri, N., Omidi, S., 2020. Enhancement the economical and environmental aspects of plus-zero energy buildings integrated with INVELOX turbines. Renew. Energy 153, 1355–1367.
Shaterabadi, M., Jirdehi, M.A., 2020. Multi-objective stochastic programming energy management for integrated INVELOX turbines in microgrids: a new type of turbines. Renew. Energy 145, 2754–2769.
Shen, Z., Gong, S., Zuo, Z., Chen, Y., Guo, W., 2024. Darrieus vertical-axis wind turbine performance enhancement approach and optimized design: a review. Ocean Eng. 311, 118965.
Shen, W.Z., Zakkam, V.A.K., Sørensen, J.N., Appa, K., 2007. Analysis of counter-rotating wind turbines. J. Phys. Conf. Ser. 75, 1–9.
Shi, L., Feng, F., Guo, W., Li, Y., 2021. Research and development of a small-scale icing wind tunnel test system for blade airfoil icing characteristics. Int. J. Rotating Mach. 1–12.
Song, D., et al., 2018a. Maximum power extraction for wind turbines through a novel yaw control solution using predicted wind directions. Energy Convers. Manag 157, 587–599.
Song, D., et al., 2018b. Power extraction efficiency optimization of horizontal-axis wind turbines through optimizing control parameters of yaw control systems using an intelligent method. Appl. Energy 224, 267–279.
Spiru, P., Simona, P.L., 2024. Wind energy resource assessment and wind turbine selection analysis for sustainable energy production. Sci. Rep. 14 (1 14), 1–16.
Srivastava, M., Maheshwari, S., Kundra, T., Rathee, S., 2017. Multi-response optimization of fused deposition modelling process parameters of ABS using response surface methodology (RSM)-based desirability analysis. Mater. Today Proc. 4, 1972–1977.
Tabatabaeikia, S., et al., 2016. Computational and experimental optimization of the exhaust air energy recovery wind turbine generator. Energy Convers. Manag 126, 862–874.
Taghinezhad, J., Alimardani, R., Masdari, M., Mahmoodi, E., 2021a. Performance optimization of a dual-rotor ducted wind turbine by using response surface method. Energy Convers. Manag. X 12, 100120.
Taghinezhad, J., Alimardani, R., Masdari, M., Mosazadeh, H., 2024. Parametric study and flow characteristics of a new duct for ducted wind turbines system using analytical hierarchy process: numerical & experimental study. Energy Syst. 15, 585–614.
Taghinezhad, J., Alimardani, R., Mosazadeh, H., Masdari, M., 2019. Ducted wind turbines a review. Int. J. Future Revolut. Comput. Sci. Commun. Eng. 5, 19–25.
Taghinezhad, J., Mahmoodi, E., Masdari, M., Alimardani, R., 2021b. Simulation and optimization of ducted wind turbines using the response surface methodology and analytical hierarchical process. 7th Iran Wind Energy Conference (IWEC2021). IEEE, pp. 1–6. https://doi.org/10.1109/IWEC52400.2021.9466971.
Tao, T., et al., 2024. Time-domain fatigue damage assessment for wind turbine tower bolts under yaw optimization control at offshore wind farm. Ocean Eng. 303, 117706.
Tayebi, A., Torabi, F., 2024. Flow control techniques to improve the aerodynamic performance of Darrieus vertical axis wind turbines: a critical review. J. Wind Eng. Ind. Aerodyn. 252, 105820.
Teng, H., et al., 2023. Carbon fiber composites for large-scale wind turbine blades: applicability study and comprehensive evaluation in China. J. Mar. Sci. Eng. 11 (624 11), 624.
Tian, L., et al., 2024. Predictive capability of an improved AD/RANS method for multiple wind turbines and wind farm wakes. Energy 297, 131207.
Visser, K.D., 2024. On the underperformance of the full-scale Clarkson University 3 meter ducted turbine. J. Phys. Conf. Ser. 2767, 072027.
Walia, A., Mehta, P., Guleria, S., Shirkot, C.K., 2015. Improvement for enhanced xylanase production by Cellulosimicrobium cellulans CKMX1 using central composite design of response surface methodology. 3 Biotech 5, 1053–1066.
Wang, Z., Ozbay, A., Tian, W., Hu, H., 2018. An experimental study on the aerodynamic performances and wake characteristics of an innovative dual-rotor wind turbine. Energy 147, 94–109.
Wang, J., Piechna, J., Müller, N., 2013. Computational fluid dynamics investigation of a novel multiblade wind turbine in a duct. J. Sol. Energy Eng. 135.
Wern, N.K. Fabrication, Testing and Performance Enhancement of a Small Scale Tidal Current Turbine. (University of Malaya Kuala Lumpur, 2016).
Yesilbudak, M., Ozcan, A., 2024. Performance comparison of Metaheuristic optimization-based parametric methods in wind turbine power curve modeling. IEEE Access 12, 99372–99381.
Yuji, O., Koichi, W., 2019. A new approach toward power output enhancement using multirotor systems with shrouded wind turbines. J. Energy Resour. Technol. 141.
Zanoun, E.S., 2018. Flow characteristics in low-speed wind tunnel contractions: simulation and testing. Alex. Eng. J. 57, 2265–2277.
Zhou, F., Yang, J., Pang, J., Wang, B., 2023. Research on control methods and technology for reduction of large-scale wind turbine blade vibration. Energy Rep. 9, 912–923.